Convergent crater circulations on Mars: Influence on the surface pressure cycle and the depth of the convective boundary layer

Citation	Tyler, D., & Barnes, J. R. (2015). Convergent crater circulations on Mars: Influence on the surface pressure cycle and the depth of the convective boundary layer. Geophysical Research Letters, 42(18), 7343-7350. doi:10.1002/2015GL064957
DOI	10.1002/2015GL064957
Publisher	John Wiley & Sons, Inc.
Version	Version of Record
Terms of Use	http://cdss.library.oregonstate.edu/sa-termsofuse

AGU PUBLICATIONS

Geophysical Research Letters

RESEARCH LETTER
10.1002/2015GL064957

Key Points:
- Crater circulations are isolated and studied with a Mars mesoscale model
- Crater circulations affect the surface pressure cycle and the depth of the mixed layer
- Similar circulations are expected across a wide range of scales and terrain types

Supporting Information:
- Texts S1–S3, Figures S1–S8, and Captions for Animations S1–S3
- Animation S1
- Animation S2
- Animation S3

Correspondence to:
D. Tyler,
dtyler@coas.oregonstate.edu

Citation:
Tyler, D., Jr., and J. R. Barnes (2015), Convergent crater circulations on Mars: Influence on the surface pressure cycle and the depth of the convective boundary layer, *Geophys. Res. Lett.*, *42*, 7343–7350, doi:10.1002/2015GL064957.

Received 15 JUN 2015
Accepted 3 SEP 2015
Accepted article online 7 SEP 2015
Published online 30 SEP 2015

Convergent crater circulations on Mars: Influence on the surface pressure cycle and the depth of the convective boundary layer

Daniel Tyler Jr.[1] **and Jeffrey R. Barnes**[1]

[1]College of Earth, Ocean, and Atmospheric Sciences, Oregon State University, Corvallis, Oregon, USA

Abstract Modeling of slope flow circulations in idealized axisymmetric craters is used to understand (1) the large surface pressure amplitude observed in Gale Crater by the Rover Environmental Monitoring Station and (2) the shallow convective boundary layer (CBL) suggested by Curiosity imagery. Air temperatures vary within craters with greater amplitudes than outside them, becoming warmer/colder during day/night. This crater circulation effect is most significant over the depth of the crater (key parameter). Within the idealized craters, a surface pressure cycle develops (in the real atmosphere it is enhanced). Partially caused by thermal expansion, a "surge" of mass away from the craters develops during daytime. Over crater floors, the CBL depth is inhibited by a capping inversion from the adiabatic warming of widespread daytime subsidence. For a variety of craters (radius, depth, and with or without a central mound), the results are very similar. In real-atmosphere simulations over canyons or large basins, similar circulations are seen.

1. Introduction

The Mars Science Laboratory (MSL) rover Curiosity began exploring Gale Crater on 5 August 2012. Observations from the Rover Environmental Monitoring Station (REMS) [*Gomez-Elvira et al.*, 2012] revealed that the surface pressure amplitude was surprisingly large. In describing the first 100 Martian solar days (sols) of REMS data, *Haberle et al.* [2014] suggest that a crater circulation plays an important role in this. Using model results produced in support of MSL, *Tyler and Barnes* [2013] (hereafter *TB2013*) describe how the topography of Gale Crater and Mount Sharp contribute in the formation of a complex crater circulation.

In studying the atmosphere of Mars, normalized surface is a useful diagnostic. It is defined as surface pressure divided by its diurnal mean: $\hat{p}_{\mathrm{sfc}}(t) = p_{\mathrm{sfc}}(t)/\overline{p}_{\mathrm{sfc}}$. When comparing locations outside Gale Crater with those inside, *TB2013* noted two important differences: (1) the range of the normalized surface pressure cycle is generally much larger inside and (2) the convective boundary layer (CBL) depth is generally much shallower inside. The good agreement between the surface pressure cycle predicted by *TB2013* and the REMS surface pressure observations suggests (1) is related to a crater circulation. Supportive of (2), imagery from the Curiosity Navigation Cameras suggests that dust devils are extremely rare and that dust settles in a more stable atmosphere [*Moores et al.*, 2015] (both suggest a shallow CBL). In the atmospheric modeling performed for the Mars Exploration Rovers, topographically forced mesoscale subsidence was seen to suppress the CBL in Gusev Crater [*Toigo and Richardson*, 2003]. Also, as described by *Rafkin and Michaels* [2003], and for another season by *Tyler et al.* [2002], the diurnal amplitude of the surface pressure cycle in Valles Marineris was found to be surprisingly large; this is almost certainly related to a canyon system circulation.

Gale Crater is located at the base of the hemispheric dichotomy, which produces a vigorous large-scale diurnal cycle of slope flow across the crater. Since Gale Crater is highly asymmetric (both in topography and albedo), the full circulation is exceedingly complex. *TB2013* suggested that the crater circulation modifies the normalized surface pressure cycle at the crater floor, doing so by making air temperatures significantly warmer/colder over a deep layer during daytime/nighttime, in contrast to locations outside the crater. On Mars (with short radiative timescales and ground temperatures generally independent of elevation), isotherms near the ground tend to align with the regional topography, causing the normalized surface pressure cycle to typically vary only slightly across a region. When a crater circulation modifies the air temperature profile, it modifies the pressure scale height profile versus height above ground level (agl). Thus, sizeable change in the amplitude of the normalized surface pressure cycle can result.

To understand these relationships, and the effect crater circulations have on the surface pressure cycle and the depth of the CBL, idealized axisymmetric craters are prescribed in a simplified version of the model of *TB2013*. Here results from one of many cases (a crater, with a central mound and a depth equal to the mean depth of Gale Crater) are described. To compare with the results of *TB2013*, these simulations are configured for MSL landing ($L_s = 151°$) at the elevation and latitude of Gale Crater, 5°S.

2. Methodology

Crater circulations are most easily studied when isolated, with atmospheric thermal tides and regional circulations removed. Our mesoscale model has been modified in four ways to accomplish this: (1) solar forcing varies identically everywhere, (2) the Coriolis force is set to zero, (3) a zero-flow condition is imposed at the lateral boundary of the mother domain, and (4) a diurnal cycle of air temperature profiles is constructed for use at the lateral boundary of the mother domain (also used for model initialization). With these changes, all model locations are at the same local time of day, and the total atmospheric mass in the mother domain cannot change during the simulations.

The diurnal cycle of air temperature prescribed at the mother domain boundary is constructed by running the model in a radiative-convective mode (with flat topography and all winds set to zero so surface pressure is constant). The resulting temperature profiles are in equilibrium with the radiative forcing when there is no variation in surface pressure. This process, the model, its configuration, and the construction of crater topographies are all described with greater detail in the supporting information.

When winds are then allowed over flat topography, the result is an almost perfectly calm atmosphere, with no diurnal variation in surface pressure. Atmospheric thermal tides are not present, and the atmosphere only expands/contracts in the vertical with the diurnal cycle. Crater topographies are introduced, the model is allowed to spin-up for two sols, the nest is activated and allowed to spin-up for one sol, and the results from the fourth sol are examined and described below.

3. Results

By design, the modeled circulation is highly symmetric with respect to the crater center. Thus, the mean axisymmetric circulation is the crater circulation. At each of 48 output times daily, 120 radial slices through the model data are averaged to construct it (the left edge of all slices is the crater center).

3.1. The Daytime Circulation

For a local solar time (LST) of 1500 h, when the maximum CBL depth is typically reached, Figures 1a–1f, respectively, show the mean axisymmetric slices of potential temperature (θ), air temperature (T), vertical wind velocity (w), radial horizontal wind velocity (U, the dot product of the unrotated wind and its radial unit vector), the nest topography, and the CBL depth. The radial wind U depicts the mature daytime phase of the circulation, which begins shortly after sunrise and develops throughout the day. Near the ground, strong flow (a "surge" away from the crater) has expanded to ~50 km beyond the crater rim. In the vertical wind field w, a strong updraft feature is seen at its leading edge. For this case, the surge expands outward another ~100 km before it fully dissipates at ~1900 h LST. The surge is maintained by and dependent on a strong horizontal pressure gradient, strongest essentially at the level of the surrounding terrain over the crater rim. The pressure gradient forms and persists due to the cooler air that exists at and above the level of the surrounding terrain over the crater floor, a structure most evident in the potential temperature θ. The surge of cooler air produces a horizontal gradient in near-surface air temperatures just outside the crater.

If we integrate the hydrostatic equation downward from a higher level (where the pressure field is flat in these idealized simulations) through the cooler air over the crater floor, the pressure at the level of the surrounding terrain is significantly greater than it is at the same level over the surrounding terrain. This outward directed pressure gradient force develops rapidly after sunrise at ~0900 h LST (see Animations S1–S3 in the supporting information). It forms as the near-surface air temperatures outside the crater rim warm in response to surface heating. As the crater circulation develops, this structure is enforced and the pressure gradient strengthens, maintaining the surge of mass away from the crater as air within the crater expands in response to the adiabatic warming of widespread subsidence in the strengthening crater circulation.

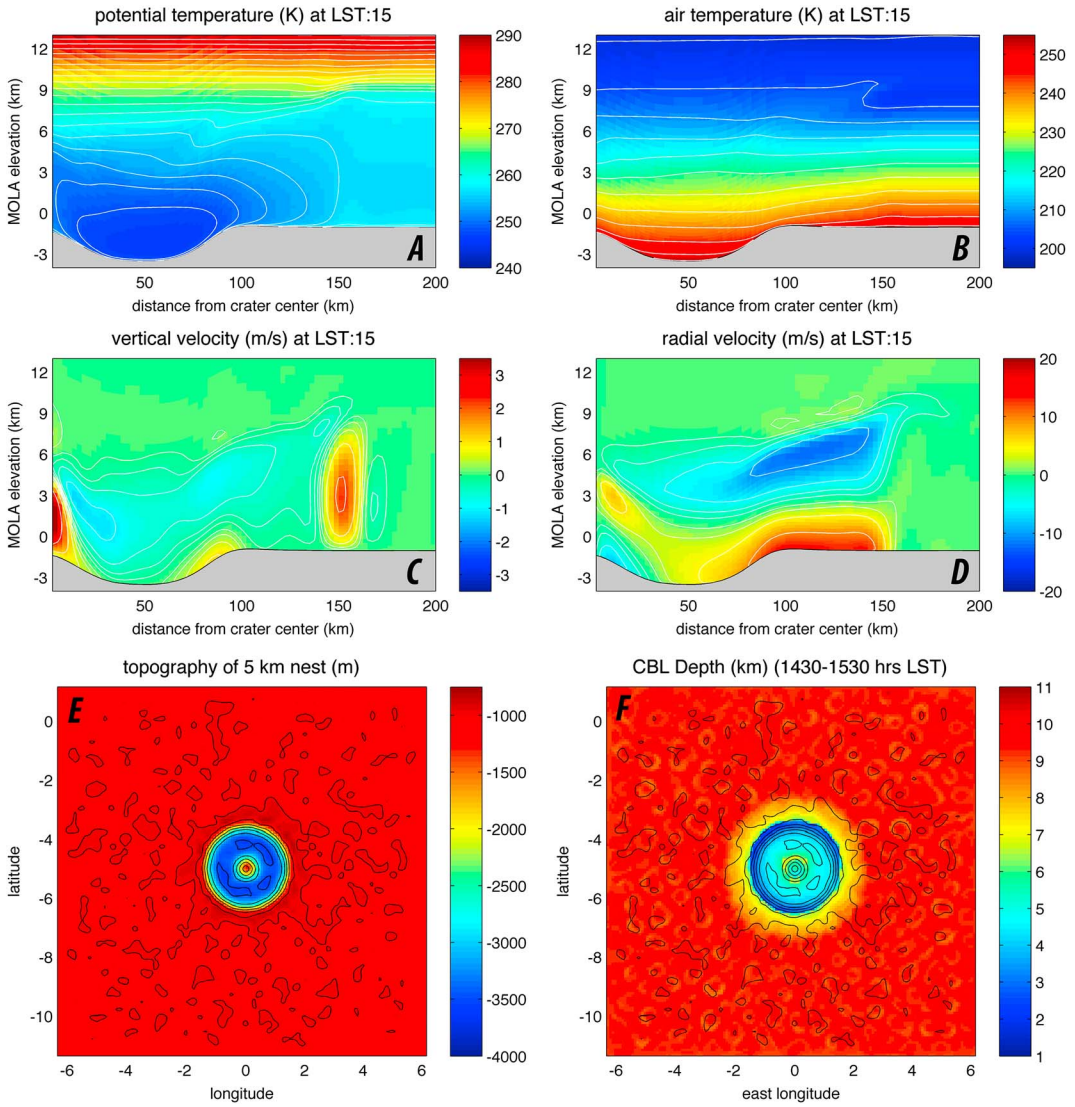

Figure 1. The mean axisymmetric circulation at 1500 h LST is shown for the case with a central mound and a crater depth of 2.5 km. (a) The potential temperature (θ; contour interval is 2 K); (b) the air temperature (T; contour interval is 5 K); (c) the vertical wind velocity (w); (d) the radial horizontal wind velocity (U); (e) the nest topography (5 km resolution) and (f) the afternoon CBL depth are shown.

Above the central mound in Figure 1, the vertical wind is quite strong, a consequence of convergent upslope flow. At the top of this plume, air flows outward and subsides over the crater floor. Strong upslope flow at the central mound and the crater walls requires return flow. This exists as widespread subsidence over the crater floor, with downward velocities of ~0.5–1.0 m/s (shades of blue in the vertical wind field w). This subsidence produces adiabatic warming and a capping inversion that strongly inhibits CBL growth. Within the crater, potential temperature begins to increase with height much nearer the ground. With this, the depth of the well-mixed layer over the crater floor (the CBL depth, where θ is constant) is much shallower than outside the crater. Regarding the depth of the CBL in Figure 1f, a structural similarity to that of *TB2013* (their Figure 5) is evident. As predicted for Gusev Crater by *Toigo and Richardson* [2003] and as simulated here, crater circulations are expected to hinder growth of the CBL.

3.2. The Diurnal Cycle of Surface Pressure

In this idealized simulation, the crater circulation produces a sizable surface pressure cycle at the floor of the crater (in the real atmosphere, a crater circulation enhances the cycle). To understand this, we consider the

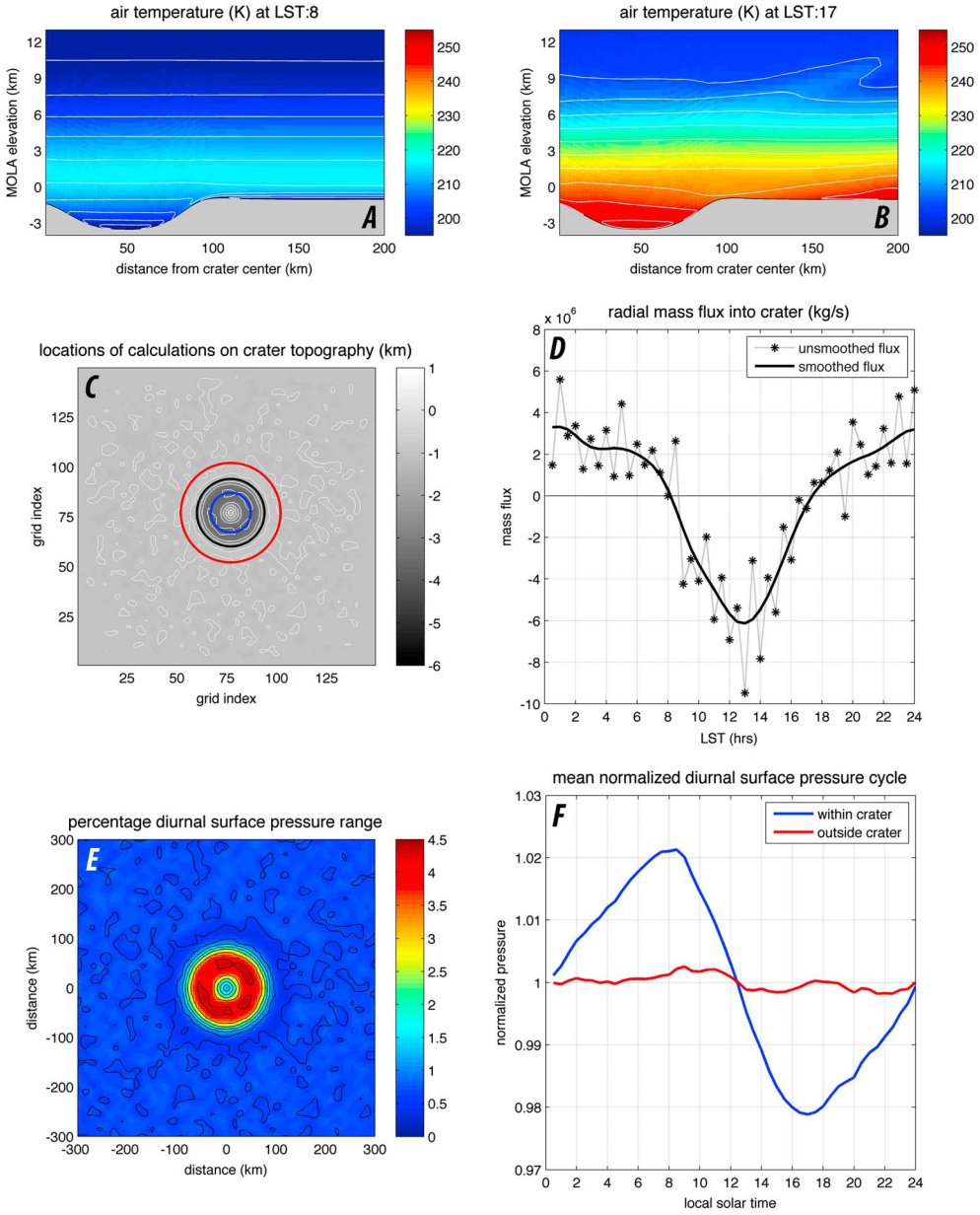

Figure 2. (a and b) Air temperature is shown at 0800 h and 1700 h LST. (c) The mass flux "cylinder" (heavy black line) is located on topography, and the heavy blue and red lines show where surface pressures are gathered to construct the mean normalized surface pressure cycles. (d) The calculated mass flux values (dashed black line with asterisks), and a smoothed result (heavy black line), are shown. (e) The range of the normalized surface pressure cycle, $100 \times \left(p_{sfc}^{max} - p_{sfc}^{min}\right)/\overline{p}_{sfc}$, is shown, and (f) the two normalized surface pressure cycles are shown (for the crater floor in blue, and ~40 km outside the crater in red).

entire diurnal cycle. The daytime surge away from the crater is a definitive clue: for a surface pressure cycle to develop inside the crater, the mass of air over the crater floor must vary diurnally, whereas even a short distance away from the crater (by design in these idealized simulations) the surface pressure amplitude is very small. The basic explanation is that air temperature profiles are only modified over the crater floor (most significantly over the depth of the crater).

To explicitly show the diurnal variation in air mass over the crater floor, the mass flux of air passing through a virtual cylinder (placed at the crater rim) is calculated at all times of day. The result in Figures 2a–2f, shows air temperatures at 0800 h LST, air temperatures at 1500 h LST, the locations of the virtual cylinder and where

two average surface pressure cycles are calculated, the mass flux, the percentage range of the normalized surface pressure cycle, and the normalized surface pressure cycles at the two locations. The "noise" in the mass flux signal is a consequence of the mother domain boundary in the model. It was carefully examined; we understand it and have mitigated it within the limitations of the model (see discussion in the supporting information). When viewed in a signal/noise context, the mass flux signal is sufficiently large to demonstrate that mass flows into the crater during nighttime (positive values), and out of the crater during daytime (negative values). At two times of day, ~0800 and ~1700 h LST, the mass flux changes sign. These times are important regarding the vertical structure of air temperature over the crater floor in comparison to locations outside the crater (locations that are unmodified by the crater circulation). For these two times, the temperature subpanels of Figure 2 show the much deeper layer of cold/warm air during the nighttime/daytime that has formed over the crater floor.

The mean normalized surface pressure cycles are shown for two locations in Figure 2f (the locations are identified in Figure 2c). Just ~40 km away from the crater the surface pressure cycle is negligible, while at the crater floor the range is large, ~4%. An amplitude of ~2% is sizeable, equivalent to or greater than typical amplitudes of the surface pressure diurnal mode. In equatorial regions the diurnal amplitude can become very large, especially when the eastward and westward modes are constructively interfering, as is believed to be the case near Gale Crater when Curiosity landed [*Haberle et al*., 2014]. It is worth noting that the 4% range simulated here (in this idealized crater simulation) is in excellent agreement with the prediction of *TB2013* (their Figure 8) that the range of the normalized surface pressure cycle at the MSL landing site would be ~4% larger than it would be just outside Gale Crater.

In the real atmosphere, when only weak convergent/divergent flow is produced by small local variations in topography (and only shallow/small craters/hills modify the regional variation), the local air temperature profiles are not modified. In this situation, the range of the normalized surface pressure cycle is surprisingly invariant across the larger-scale region. If we examine high-resolution results from a regional mesoscale model with sizable smaller-scale terrain variations, the range of the normalized surface pressure exhibits sizable highs and lows that correlate with the smaller-scale variability. When wind fields are examined, convergent/divergent flow is associated with these smaller-scale features. The convergent/divergent part of the flow can modify the air temperature profile near the ground (over a depth that scales with the smaller-scale features themselves). Over more gradual and larger-scale regional terrain variations (such as with parts of the hemispheric dichotomy near Gale Crater) the variation can be surprisingly small. As a diagnostic, normalized surface pressure is useful in identifying terrain that has significantly affected the local flow and air temperature profiles.

3.3. The Air Temperature Profile and the Crater Circulation

The greatest modification of air temperature profiles over the crater floor (compared to outside the crater versus height agl) is seen twice daily, at ~0800 and ~1700 h LST (Figures 2a and 2b). At these times, when atmospheric isotherms tend to be horizontal above the crater floor in alignment with the flat terrain of the region instead of the topography of the crater, the surface pressure at the crater floor is at its respective maximum/minimum values (Figure 2f). The crater circulation eliminates horizontal gradients that would otherwise exist if the diabatic forcing were only radiative-convective (causing the isotherms to then follow all terrain variations). By modifying air temperature profiles over the depth of the crater, the convergent/divergent component of the circulation plays an important role.

At ~0800 h LST, after cold-air pooling has been the primary dynamic component for many hours, isotherms are in alignment with the regional topography (not that of the crater). As a result, the pressure scale height profile over the crater floor is significantly different from that over the surrounding plains (similarly so at ~1500 h LST). Quite basically, it is the modified pressure scale height profile that produces a surface pressure cycle at the crater floor in these idealized simulations. Elsewhere, as evident in Figure 2e, the surface pressure (and thus the amount of mass in the air column) varies only minimally. At the lowest elevations of the crater in Figure 2e (correlated with the contours of topography), we find the greatest values of the percentage diurnal range of the normalized surface pressure. This strong correlation is a consequence of the surface pressure effect being very dependent on the depth of the crater, a sensitivity that is shown in the supporting information for a crater half as deep. Outside the crater (specifically outside the effect of the circulation), we note that similar small-scale terrain variations do not produce a similar effect in the range of the normalized surface pressure.

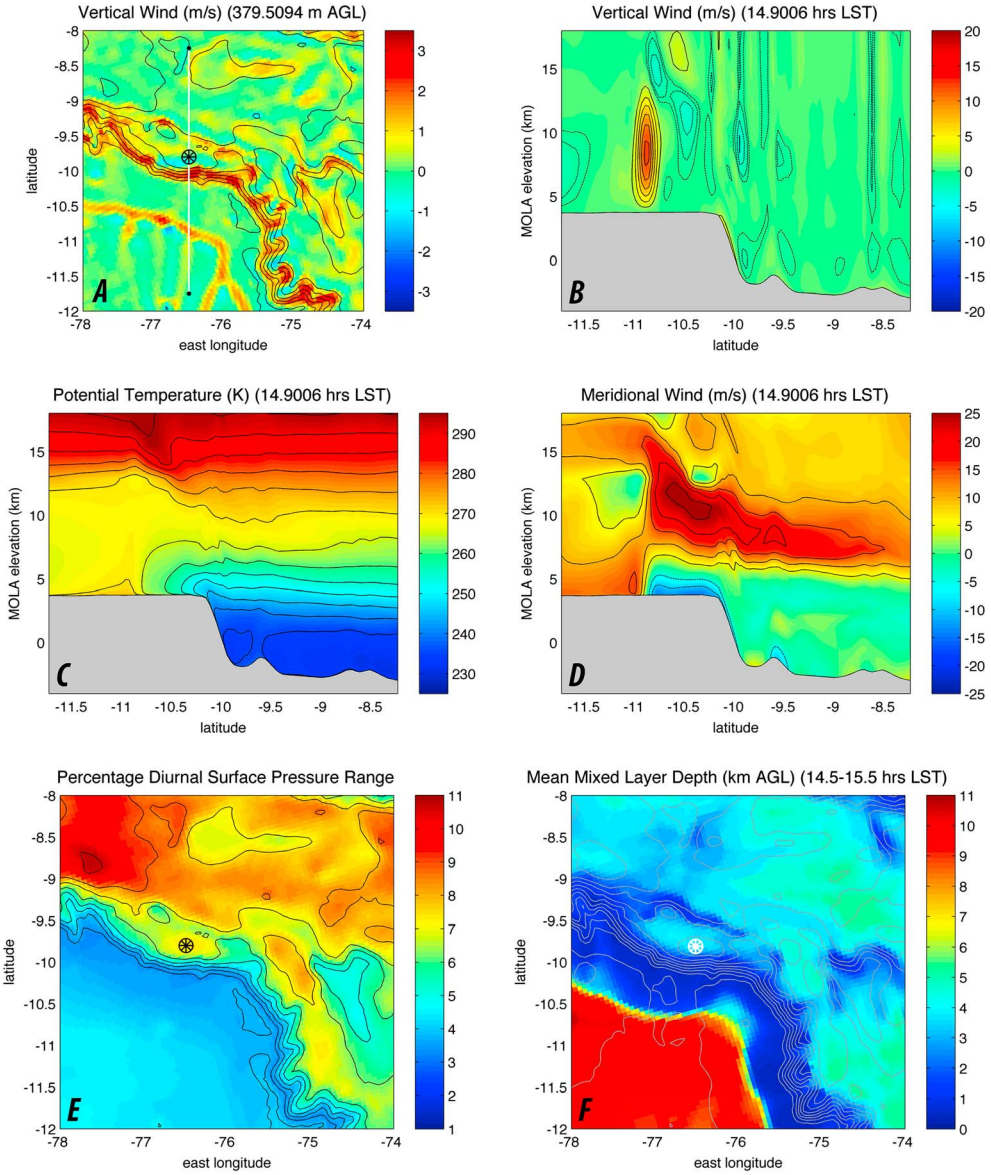

Figure 3. Results are shown for a Melas Chasma simulation at $L_s = 5°$, a possible Mars 2020 landing site (the circled asterisks in Figures 3a, 3e, and 3f. The topography is contoured at 1 km intervals. For a subset of the highest resolution nest (4 km), (a) the vertical wind near the surface (strong upslope flow) is shown. The white line segment in Figure 3a is the surface transect of the vertical slices of data shown in Figures 3b–3d. (b–d) Instantaneous vertical slices of vertical wind (w), potential temperature (θ), and meridional wind (v). (e and f) The percentage range of the normalized surface pressure cycle and the afternoon CBL depth (~1500 h LST).

In the absence of air temperature observations with sufficient vertical resolution, both inside and outside of target craters, the REMS surface pressure observations (along with the modeling described here) lead to the conclusion that crater circulations should be suspected of modifying air temperature profiles within craters as simulated here. By using prescribed temperature profiles (or pressure scale height profiles), the hydrostatic equation can be numerically integrated in the vertical to calculate the change in the air column mass below some height agl, and thus quantify the change in the normalized surface pressure cycle. For the interested reader, an example that is consistent with this idealized crater case is provided and discussed in the supporting information.

3.4. Other Crater Topographies and Real-Atmosphere Analogues

Simulations with other crater topographies (for diameters both smaller and larger, with or without central mounds) yield very similar results. When there is no central mound, the crater circulation is less complex,

although little change is seen in the surface pressure cycle at the crater floor (supporting information includes this case). With no crater there can be no effect, which makes the crater depth a controlling factor. For a crater half as deep the surface pressure cycle is half as large (supporting information includes this case). For very large craters, the afternoon minimum surface pressure tends to occur somewhat later, with a lessened afternoon decrease that appears to be sensitive to the existence of a central mound. For very large and shallow craters without central mounds, the crater circulation is weak, and its effect is likely to be mitigated by other circulations in the real atmosphere.

Based on this initial investigation, our results are not that sensitive to scale (additional study is warranted). If dynamically similar effects exist across a wide-scale range, then topography that produces convergent/divergent circulations should correlate with modified air temperatures near the ground that affect the surface pressure cycle and the depth of the CBL. When high-resolution mesoscale model results are examined, this correlation tends to be seen. A lot of structure (sharp gradients) is seen in the amplitude of the normalized surface pressure cycle and the depth of the CBL, structure that tends to be correlated with the smaller-scale or sharper features of the terrain in the region. If similar dynamics have a role across a wide-scale range, we would expect to find "surges" expanding away from a great many topographical features on Mars.

Melas Chasma provides a fascinating case study for mesoscale modeling, and this discussion can be advanced upon examining results from a Melas Chasma simulation performed with the present version of the model of *TB2013* (employed to study candidate sites for the NASA Mars 2020 mission). At ~1500 h LST for the landing season (L_s=5°), a vigorous afternoon circulation is depicted in Figure 3. In comparing this real-atmosphere simulation to the idealized simulations of this study, important similarities between the very different cases are seen.

For orientation (Figure 3a), the vertical wind near the surface is shown on contours of topography for a subset of the model nest (the white line is the surface transect of the vertical slices of data shown in Figures 3b–3d). In comparison to Figure 1, although for a far more complex circulation, similar features are evident. Strong flow up the Melas Chasma wall is seen in Figures 3a, 3b, and 3d, with a surge away from the canyon rim seen at the surface in the meridional wind in Figure 3d. At the leading edge of the surge (~10.9°S in Figures 3b–3d), the similarity with the features in Figure 1 is most evident. The potential temperature in Figure 3c suggests a strong horizontal pressure gradient force (directed to the south), with a deep layer of cooler air advancing to the south. At the leading edge of the surge, a very strong feature is seen in the vertical wind field in Figure 3b. The spatial location of the leading edge of this noncircular surge is seen in Figure 3a (it is crossed by the surface transect about ¼ into each slice from the left). Also, the normalized surface pressure range (Figure 3e) is much larger at the floor of Melas Chasma than it is outside the canyon to the south, and the CBL depth (Figure 3f) is dramatically shallower inside the canyon (presumably in response to widespread subsidence, with many pockets of sizable subsidence visible over the canyon floor in Figure 3b). Qualitatively, these aspects of the circulation are quite similar to the crater circulation of Figures 1 and 2. Quite possibly, with curves and bends along steep gradients of topography across Mars, the convergent/divergent component of the circulation is regularly involved in the local surface pressure cycle and the depth of the CBL. And if so, then the superposition of multiple surges is a mechanism at the mesoscale that could play an important role.

4. Concluding Discussion

Idealized mesoscale model simulations (without atmospheric tides) are used to isolate and investigate crater circulations. Widespread daytime subsidence over crater floors produces adiabatic warming. This warming inhibits growth of the CBL by forming a capping inversion and contributes in producing a surface pressure cycle when otherwise there is none. Crater circulations are not mass conserving. During daytime, a surge of mass away from the crater develops as the atmosphere over the crater floor becomes warmer more deeply than it does over the surrounding plains. At night convergent katabatic flow fills the crater with cold air (cold-air pooling), with upwelling and adiabatic cooling helping to produce a deeper cold layer than over the surrounding plains. When compared with the surrounding plains, the vertical profile of air temperature over the crater floor is modified most significantly when the surface pressure is at its maximum/minimum in the A.M./P.M. (respectively, ~0800 and ~1700 h LST). At these two times of day, the mass flux of air into the crater reverses sign. In comparison to locations outside the crater, it is the modified air temperature profile that explains the surface pressure cycle in these idealized simulations. That this forcing is generally in phase with the unmodified

diurnal cycle of surface pressure on Mars serves to explain the surprisingly large surface pressure cycle observed by REMS. The ~4% normalized surface pressure range found in this study (caused only by the crater circulation) agrees with what *Haberle et al*. [2014] and *TB2013* attribute to the crater circulation in Gale Crater. The good agreement from this study is importantly dependent on the idealized crater being configured with a depth equivalent to that of Gale Crater at the MSL landing site, ~2.5 km. With a crater half as deep, the effect is half as large (see additional results in the supporting information). The depth of the crater is a controlling parameter.

If we consider widely separated locations at different elevations (in the same region) on Mars, regardless of whether the terrain is high or low, the air temperatures at some height agl (near the ground) are quite similar in the absence of a crater circulation. If horizontal separation distances are short (steep slopes), strong slope flow develops. If the slope flow is respectively convergent/divergent during the nighttime/daytime (a crater circulation), the local radiative-convective tendency of isotherms to orient with the terrain on Mars is modified. This changes the pressure scale height profile near the surface and can cause sizeable spatial variation in the range of the normalized surface pressure cycle (variation that otherwise tends to be small). On Mars, slope flows are prolific, and with steep slopes that trace curving arcs across the planet, the resulting convergent/divergent circulations will modify the expected diurnal variation of air temperature versus height agl, causing many locations to be good subjects for further investigation.

As observed by *Hinson et al*. [2008] and modeled by *Spiga et al*. [2010], CBL depths tend to correlate with variations in the larger-scale topography. Along with the "pressure effect" described by *Spiga et al*. [2010], they discuss how mesoscale circulations may be responsible for differences between some of their simulations and the observations. This study addresses that specific aspect of a very complex relationship, describing how crater circulations (and mesoscale circulations, in general) can dramatically affect the depth of the CBL. Considering even larger spatial scales, mesoscale models predict smaller CBL depths over a large fraction of Isidis Planitia (as do global climate models or GCMs), while simultaneously predicting greater depths at similar terrain heights into Utopia Planitia.

For large basins (even a semiclosed basin such as Isidis Planitia), we suspect that slope flows are able to produce a convergent/divergent circulation capable of influencing CBL development. As part of a much larger-scale and complex canyon circulation, the Melas Chasma results examined here reveal important dynamic similarities with crater circulations at much smaller scales. Quite possibly, the importance of these types of circulations in the atmosphere of Mars has been poorly considered. One aspect of these circulations deserving of further study would be the interaction between surges that expand away from the features that have produced them. In regions of high crater density, the mesoscale dynamics of such interaction (unresolved in GCMs) would be expected to enhance vertical mixing, which would be climatologically significant.

Acknowledgments

We would like to thank Robert M. Haberle and Alexandre M. Kling for many useful discussions regarding their similar study. Also, we want to thank the reviewers (David Kass and Michael A. Mischna) for comments and suggestions that improved the manuscript. The mesoscale modeling results (data) described herein will be made available upon request.

The Editor thanks Michael Mischna and David Kass for their assistance in evaluating this paper.

References

Gomez-Elvira, J., et al. (2012), REMS: The Environmental Sensor Suite for the Mars Science Laboratory Rover, *Space Sci. Rev.*, *170*, 583–640, doi:10.1007/s11214-012-9921-1.

Haberle, R. M., et al. (2014), Preliminary interpretation of the REMS pressure data from the first 100 sols of the MSL mission, *J. Geophys. Res. Planets*, *119*, 440–453, doi:10.1002/2013JE004488.

Hinson, D. P., M. Pätzold, S. Tellmann, B. Häusler, and G. L. Tyler (2008), The depth of the convective boundary layer on Mars, *Icarus*, *198*(1), 57–66, doi:10.1016/j.icarus.2008.07.003.

Moores, J. E., et al. (2015), Observational evidence of a suppressed planetary boundary layer in northern Gale Crater, Mars as seen by the Navcam instrument onboard the Mars Science Laboratory rover, *Icarus*, *249*, 129–142, doi:10.1016/j.icarus.2014.09.020.

Rafkin, S. C. R., and T. I. Michaels (2003), Meteorological predictions for 2003 Mars Exploration Rover high-priority landing sites, *J. Geophys. Res.*, *108*(E12), 8091, doi:10.1029/2002JE002027.

Spiga, A., F. Forget, S. R. Lewis, and D. P. Hinson (2010), Structure and dynamics of the convective boundary layer on Mars as inferred from large-eddy simulations and remote-sensing measurements, *Q. J. R. Meteorol. Soc.*, *136*, 414–428, doi:10.1002/qj.563.

Toigo, A. D., and M. I. Richardson (2003), Meteorology of proposed Mars Exploration Rover landing sites, *J. Geophys. Res.*, *108*(E12), 8092, doi:10.1029/2003JE002064.

Tyler, D., and J. R. Barnes (2013), Mesoscale modeling of the circulation in the Gale Crater region: An investigation into the complex forcing of convective boundary layer depths, *Mars*, *8*, 58–77, doi:10.1555/mars.2013.0003.

Tyler, D., Jr., J. R. Barnes, and R. M. Haberle (2002), Simulation of surface meteorology at the Pathfinder and VL1 sites using a Mars mesoscale model, *J. Geophys. Res.*, *107*(E4), 5018, doi:10.1029/2001JE001618.